THERMAL DEGRADATION OF POLYMERIC FOAM CORE MATERIALS FOR SANDWICH STRUCTURES

S.Zhang[1*], J.M. Dulieu-Barton[1], R.K. Fruehmann[1], O. T. Thomsen[2]
[1] School of Engineering Sciences, University of Southampton, Highfield, SO17 1BJ, UK
[2] Department of Mechanical and Manufacturing Engineering, Aalborg University,
DK-9220 Aalborg East, Denmark
* Corresponding author (sz2g09@soton.ac.uk)

Abstract

A new methodology is proposed to characterise the shear properties of polymeric foam core materials at elevated temperature. The focus is to determine the shear modulus of the foam using strains derived from digital image correlation (DIC). Uncertainties related to the shear strain distribution in the test specimens, the test machine/rig alignment, image acquisition for the DIC and the data processing to obtain the strain are investigated. Tests are conducted at ambient temperature and in a temperature-controlled chamber at temperatures ranging from 25°C to 90°C. The foam material, Divinycell PVC H100, which is orthotropic, has a through-thickness Young's modulus approximately twice that of the value in the in-plane directions. In this paper the shear properties are studied and a similar ratio of through-thickness to in-plane behaviour is determined. The reduction in shear modulus over the temperature range agrees well with that of the tensile and compressive moduli derived in previous work. A general formulation is proposed to describe the thermal degradation of the foam core material.

Keywords: DIC, polymeric foam core materials, thermal degradation

1 Introduction

Polymeric foam cored sandwich structures are widely used in the transportation, aerospace, maritime, wind turbine and building industries [1]. Sandwich structures are often subjected to elevated temperatures, usually caused by the environment in which they are situated. For instance, due to solar radiation the surface temperature of wind turbine blades can be over 80ºC [2]. Polymer materials (e.g. PVC, PET) show significant degradation in their performance at elevated temperatures. This is manifested by a significant loss of stiffness as well as increasing influence of viscoelastic effects with rising temperature. Recently, it was found that under certain circumstances the load-response of sandwich structures may shift from being linear and stable to nonlinear and unstable due to the core material thermal degradation [3]. Even so, little attention has been paid to the performance of sandwich structures subjected to elevated temperatures. This is because the thermal-mechanical interaction is not well understood and there is a lack of material property data for polymeric foam core materials at elevated temperatures. The present paper therefore focuses on developing a reliable methodology to characterise the mechanical properties of polymeric foam materials at a range of elevated temperatures.

2 Methodology

For sandwich structures subjected to bending loading, the core mainly carries the transverse shear stress, while the face sheets carry the normal stresses forming the global bending couple. The deflection of the sandwich structure is strongly dependent on the core shear stiffness. Therefore, the present paper investigates the thermal degradation of the elastic shear properties of polymeric foam core materials. The work here is an extension of previous work by the authors [4], where the thermal degradation of the tensile and compressive Young's moduli are characterised. An optical non-contact deformation measurement based on DIC (digital image correlation) is utilised to obtain the full-field strain data. Finite element (FE) analysis is used to investigate the strain distributions in the specimen and inform the measurement methodology. The orthotropic behaviour of polymeric foam materials is established at room temperature (25°C). The shear modulus in the through-thickness direction is

obtained over a temperature range from 25°C to 90°C.

3 Specimen and experimental apparatus

Divinycell H100 PVC foam was used in this study. This is a closed-cell cross-linked foam with a nominal density of 100 kg/m^3 manufactured by DIAB. The bulk material is supplied in the form of a sheet with a thickness of 65 mm. The through-thickness direction of the foam sheet is denoted as 1, and the in-plane directions are denoted as 2 and 3, respectively. The properties in the 2 and 3 directions can be assumed identical because of the same elongation process during manufacture. Specimens were cut from the centre of the foam sheet. Both the through-thickness (plane 1-2 and 1-3) and in-plane (plane 2-3) shear properties were investigated.

The experimental apparatus is shown in Fig. 1. A lap shear fixture was designed according to ASTM standard C273/M-07. The shear fixture was enclosed in a thermal chamber (Instron EC2061) so that the specimen could be heated to the target temperature. A servo-hydraulic test machine (Instron 8502), fitted with a 5 kN load cell and 100 kN actuator, was used to load test specimens. The load was applied through two universal joints with spherical bearings that are connected to the test machine through holes in the top and bottom of the chamber. The foam specimen has dimensions of 10 mm wide × 30 mm thick × 100 mm long ($x \times y \times z$), and was bonded between two rigid steel plates (15 mm thick). The loading fixture was aligned so that the line of action of the load passes through the diagonally opposite corners of the foam specimen. The set-up promotes a close to uniform, and almost pure shear stress state in the central area of the specimen. Here, if the x-z plane is the material plane 1-2, the through-thickness shear property of the material is studied; if the x-z plane is the material plane 2-3, the in-plane shear property is studied.

A LA Vision VC-Imager E-lite digital camera with 5 mega-pixel resolution and 12 bit grayscale range was used to capture the specimen surface images during the specimen deformation process. The specimen was viewed through an optical window mounted in the door of the thermal chamber. The specimen surface was lightly coated with random white-black speckles forming a unique, high contrast pattern. Images and load cell data were collected simultaneously at a frequency of 1 Hz. The strain over the measurement area, which is selected as the central 8 × 20 mm ($x \times z$) area on the specimen surface, was obtained by image correlation using the commercial software Davis 7.4.

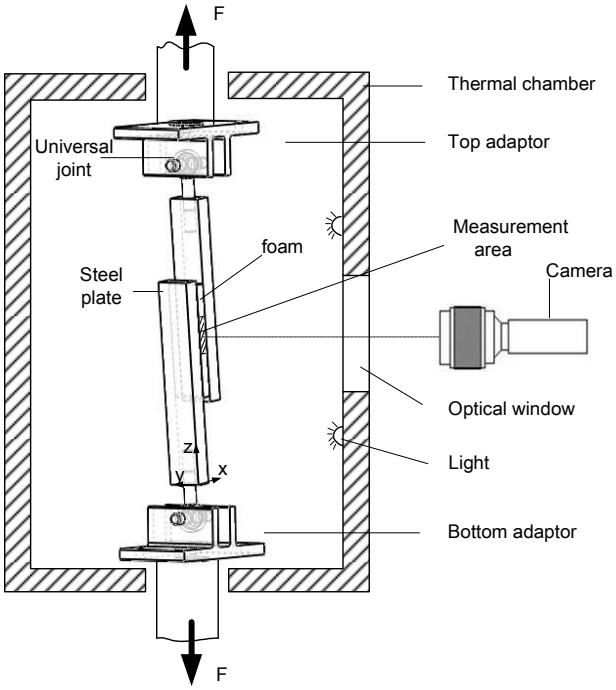

Fig. 1. Schematic of foam shear test apparatus

4 Finite element (FE) analysis

A linear elastic and small displacement FE model was constructed to study the strain distribution in the specimen, using ANSYS 12.0. The foam volume was modelled using 1 × 1 × 1 mm SOLID185 8 node orthotropic linear strain elements, while the two steel plates were modelled using 1 × 1 × 1 mm SOLID45 8 node isotropic linear strain elements. The material properties applied for the foam and steel are listed in Table 1 [4, 5].

Table 1: Material properties of FE model

Material	E_1 (MPa)	E_2 (MPa)	E_3 (MPa)	ν_{12}	ν_{23}
Foam	130	65	65	0.40	0.40
Steel	210000	-	-	0.32	-
	G_{12} (MPa)	G_{13} (MPa)	G_{23} (MPa)		
Foam	35	35	20		

A z-direction load of 1 kN was introduced to the central node of the upper surface of the upper steel plate, while the central node of the lower surface of

the lower steel plate was fixed. Both the through-thickness and in-plane shear were modelled.

The shear strain (γ_{xz}) distribution of the through-thickness shear specimen obtained from the FE analysis is shown in Fig. 2. In Fig. 2(a), the upper quadrant of the specimen and the rig has been removed to show the strain distribution across the width of the specimen. The rectangular area enclosed with dashed lines, designated as 's', represents the measurement area. To quantify the strain distribution, values of γ_{xz} along lines a, b and c are depicted in Fig. 2(b). From line b, it is seen that γ_{xz} is distributed uniformly over the measurement area. The values of γ_{xz} on the top and bottom of the specimen free surfaces should be 0, but a value of about 0.002 was derived from the FE model. This is caused by the mesh in the region not being fine enough to capture the reduction to zero. However, these edge effect have negligible influence on the measurement area. From line c, it is shown that the strain on the surface of the specimen is identical to that inside the specimen. The average value of γ_{xz} in the measurement area is obtained as 9.47 x 10^{-3} from the FE solution, which is less than 1% different from the volume average shear strain (calculated as τ_{xz} divided by G_{xz}). By constructing FE models with the same dimensions but with different foam material properties, it was found that the shear strain distribution is practically independent of the polymeric foam material properties. Therefore, a surface measurement can be used to provide an accurate representation of the volume average shear strain. For the in-plane direction shear model, a practically identical solution was obtained.

5 Strain measurement

The strain on the surface of the specimen was obtained using DIC. In DIC, displacements are tracked through the correlation of the grey scale pattern between deformed and reference images. The strain is determined from the spatial gradient of the displacement vectors derived from the correlation algorithm. The non-contacting nature of the approach ensures that the sensors are isolated from the thermal effects. As full-field data is obtained it is possible to extract both the shear and the normal strains. This allows an evaluation of the strain state in the specimen and establishes if the applied load is producing a state of pure shear in the specimen.

In DIC it is necessary to divide the image into subsets (or facets) comprising an area of pixels. This way the displacement of a feature can be tracked within each subset and the displacement vector is obtained. Appropriate subset size selection is extremely important for an accurate deformation measurement. Generally, subsets of larger sizes introduce better displacement resolution but poorer spatial resolution. A suitable subset size depends heavily on the speckle size, image contrast and correlation algorithm. To select an appropriate subset, different sizes of subsets were used to calculate the average shear strain in the measurement area, while the specimen was subjected to volume average shear stresses of 0.1 MPa, 0.3 MPa and 0.5 MPa. A convergence of the strain value was observed when the subset was 64 × 64 pixels, thus 64 × 64 pixels was deemed the most suitable.

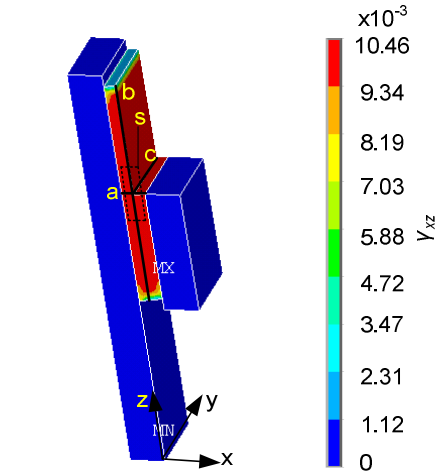

(a)

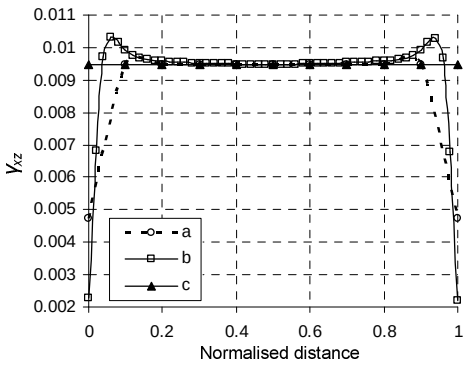

(b)

Fig. 2. FE analysis results: Distribution of γ_{xz} in the foam specimen (a) over the volume; (b) along line a, b and c

Fig. 3 shows the displacement and shear strain distributions in the measurement area obtained using DIC. Fig. 3(a) shows the full-field shear strain map (background) overlaid with the full-field displacement vectors. The values of γ_{xz} along the lines a and b are plotted in Fig. 3(b), which shows that γ_{xz} is uniformly distributed over the measurement area, with a strain measurement scatter of about 2×10^{-4}. Fig. 4 shows the average shear and normal strain components obtained from the measurement area plotted against shear/normal stress in the specimen volume. It can be seen that γ_{xz} increases proportionally with the stress, while the normal strains ε_{xx} and ε_{yy} are virtually 0 and vary negligibly with the stress. Thus, it is demonstrated that a state of pure shear is developed.

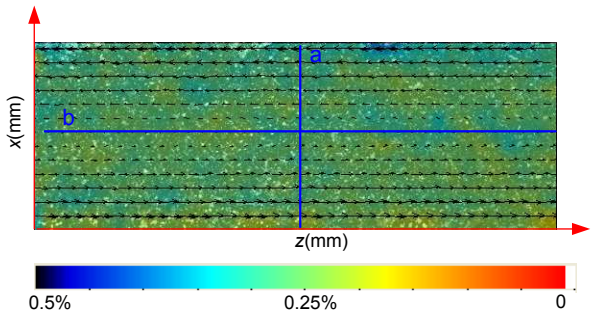

(a)

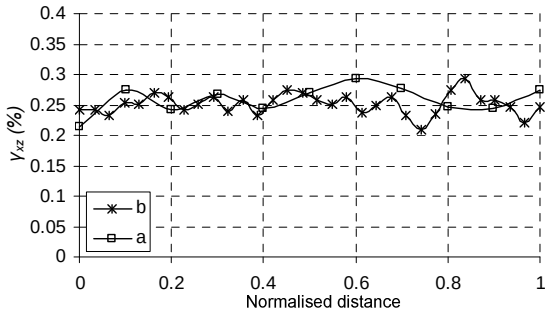

(b)

Fig. 3. Displacement and shear strain γ_{xz} measured by DIC; (a) displacement and strain distribution (b) shear strain on line *a* and *b*

The data in Figs. 3 and 4 shows that a uniform pure shear deformation state occurs in the measurement area. The FE analysis shows that there is no difference between the surface and internal shear strain. Therefore, the shear modulus G_{xz} can be derived from the linear fitting of the volume average stress (τ_{xz}) and the average shear strain (γ_{xz}) obtained from the measurement area. The standard deviation (*STD*) of G_{xz} can be calculated as:

$$STD = \frac{\sqrt{1/R^2 - 1}}{N - 2} \quad (1)$$

where N is number of data points and the R^2 value is the linear correlation coefficient. For the data given in Fig. 3, the shear modulus G_{xz} is derived as 30.23 ± 0.02 MPa, i.e. approximately 1% scatter.

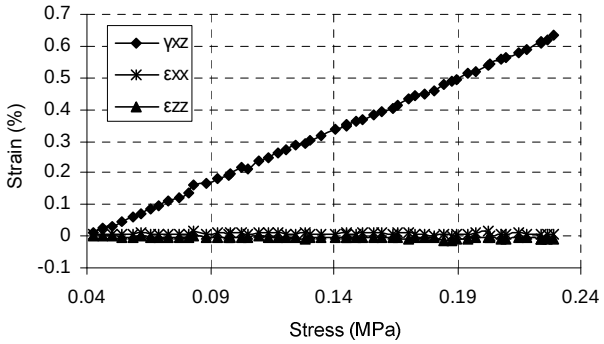

Fig. 4. Strain components in the measurement area

To evaluate the test rig alignment, an experiment was performed that compared the strain value on the front and back surfaces of the specimen. In this procedure, the thermal chamber was removed and another camera was positioned to view the back side of the specimen. Care was taken to ensure that this camera was symmetrical with the front side camera and about the specimen axes. The front and back surface images were captured simultaneously. The through-thickness shear modulus derived using the front and back surface strains is shown in Fig. 5.

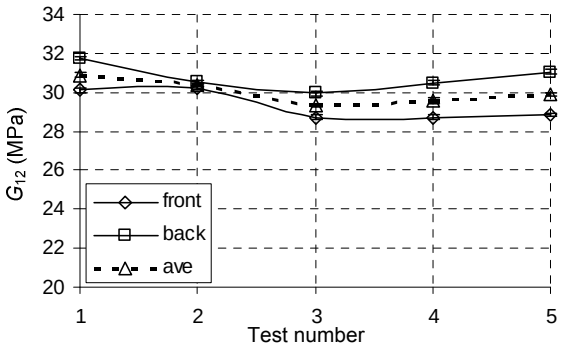

Fig. 5. Through-thickness shear modulus derived from strain on the front and back surfaces

The difference between the front and back values is negligible, which indicates that the universal joint (see Fig. 1) is accounting for any misalignment in

the test machine. Hence, it is acceptable to derive the shear modulus from images captured from only one side of the specimen.

6 Test results

Firstly, shear tests were performed at room temperature (25°C), in both the material through-thickness and in-plane directions. For a foam specimen with an average density of 88.2 kg/m^3, the through-thickness shear modulus (G_{12}) was evaluated as 30.02 ± 0.63 MPa and the in-plane shear modulus (G_{23}) was 18.28 ± 0.28 MPa. The shear modulus exhibits a similar orthotropic behaviour as that of the tensile and compressive moduli [4]. Therefore, it can be concluded that the in-plane Young's and shear moduli are approximately 50% of that in the through-thickness direction for Divinycell H100 foam.

For shear tests at elevated temperatures, images from the specimen surface were captured through the optical window mounted in the chamber door. Therefore an experiment was conducted to investigate the influence of the window on the image quality and contrast. Here, a long and thin aluminium sheet specimen was loaded in tension in the thermal chamber. The front surface of the specimen was coated with similar speckles as the foam specimen, while the back surface had a strain gauge (VISHAY EA-13) bonded to it. Surface images of the test specimen were captured through the optical window and without the optical window. The strain gauge data were collected simultaneously with the image capture. The Young's moduli of the aluminium specimen derived from the three different approaches are listed in Table 2. It is seen that the difference of the values measured with and without the optical window is approximately 2%, and both approximately equal to that obtained with the strain gauge. This demonstrates that the optical window has a negligible influence on the 2D-DIC.

Table 2. Young's modulus derived with different strain measurement

With window	Test 1	Test 2	Test 3
E_DIC	64.66±1.83	66.75±1.42	63.00±1.63
E_strain gauge	65.35±0.02	65.38±0.03	65.45±0.03
Without window	Test 4	Test 5	Test 6
E_DIC	64.39±0.78	66.25±0.56	65.54±0.76
E_strain gauge	65.50±0.03	65.71±0.02	63.92±0.03

All unit in GPa

Shear tests were then conducted on the foam at elevated temperatures over the range 25 - 90°C with an increment of 5°C. Only the through-thickness shear modulus G_{12} was considered which is of primary concern for sandwich structures. Between each temperature increment, 30 minutes were allowed to permit a uniform temperature throughout the specimen. Two specimens S1 and S2 with densities 95.1 kg/m^3 and 88.2 kg/m^3, respectively, were tested. The test results are shown in Fig. 6. A good repeatability is shown as two very similar degradation paths are exhibited. It is observed that G_{12} degrades approximately linearly with the temperature between 25°C to 75°C. Above 75°C, which coincides with the glass transition temperature (80°C) of the PVC material, a significant reduction in the shear modulus occurs. At 90°C, more than 50% of the shear modulus is lost in comparison with the room temperature value. The overall thermal degradation trend of the shear modulus is very similar to that of the tensile and compressive moduli [4] as shown in Fig. 7, where E_{t1} and E_{c1} denotes the through-thickness tensile and compressive Young's moduli, respectively. Therefore, a master curve can be proposed to describe the thermal degradation of the foam moduli. The linear region of the thermal degradation can be expressed as follows:

$$E(T) = E(T_0) * [1 - 0.006(T - T_0)] \quad T, T_0 < 75^o C \qquad (2)$$

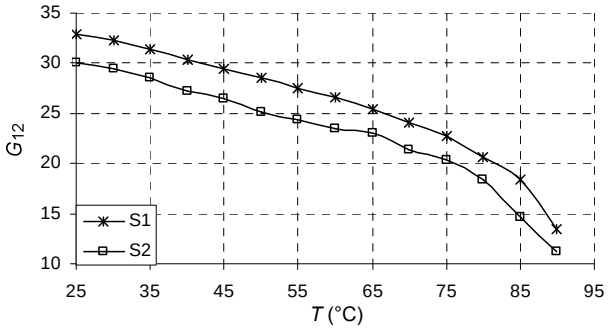

Fig. 6. Thermal degradation of G_{12} for Divinycell H100

For cellular structural materials such as polymeric foams, the material behaviour depends on both the cell wall properties and the cell structure. Although the cell structure deforms in different manners in tension, compression and shear, the thermal degradation path of the normal and shear moduli are almost identical. This indicates that the thermal degradation of foam mechanical properties is

dominated by the loss of the cell wall stiffness. Hence, it can be expected that foams of the same base polymer material but of different relative densities (e.g. Divinycell H100, H130) will degrade similarly. To validate this assumption, Divinycell H100, H130 and H200 foams, which are formed using the same base polymer but different relative densities, were tested in tension [4]. The results are shown in Fig. 8. It can be seen that the three foam materials follow the same thermal degradation path.

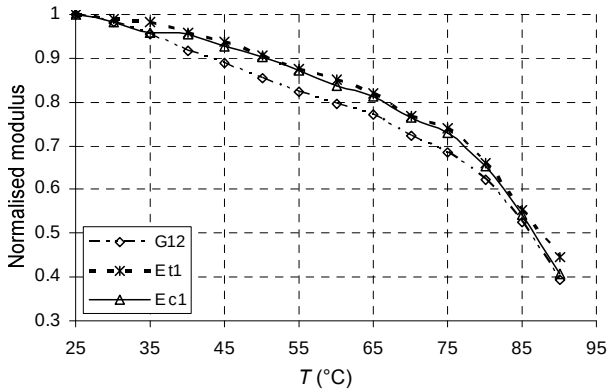

Fig. 7. Thermal degradation of through-thickness tensile, compressive and shear modulus of Divinycell H100 foam

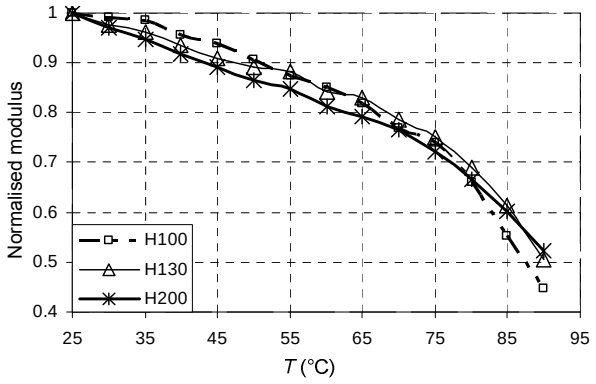

Fig. 8. Thermal degradation trend of moduli for different density foams

8 Conclusions

A methodology was proposed to characterise the shear modulus of polymeric foam core materials at elevated temperatures using DIC. To minimise uncertainties in the derived shear modulus, the methodology considers the strain distribution, specimen alignment, subset selection and the influence of the optical window on 2D-DIC. The main conclusions are as follows:

1. The lap-shear fixture can introduce a satisfactory uniform pure shear deformation state in the specimen in the elastic region, and the shear strain on the surface is the same as that throughout the specimen volume.
2. The optical window mounted in the thermal chamber has a negligible influence on the 2D-DIC.
3. The shear modulus degrades with the same path as the tensile and compressive moduli for Divinycell PVC H100 foam. The moduli decreases linearly with temperature up to 75°C, and steep reduction occurs after 75°C.
4. Foam materials with the same base polymer material but different densities follow the same thermal degradation path.

Acknowledgements

The work presented is co-sponsored by the Chinese Scholarship Council, the Danish Council for Independent Research |Technology and Production Sciences (FTP), Grant Agreement 274-08-0488, “Thermal Degradation of Polymer Foam Cored Sandwich Structures”, and the US Navy, Office of Naval Research (ONR), Grant Award N000140710227. The ONR program manager is Dr. Yapa D. S. Rajapakse. The financial support received is gratefully acknowledged.

References

[1]. D. Zenkert, *The Handbook of Sandwich Construction*. 1997: EMAS/Engineering Materials Advisory Services Ltd.

[2]. DATAFORTH. Wind Turbines Today Enhanced Reliability with Dataforth Signal Conditioners. 2010 [cited 2010 03 November].

[3]. Y. Frostig and O.T. Thomsen, Non-linear thermal response of sandwich panels with a flexible core and temperature dependent mechanical properties. Composites Part B: Engineering, 2008. 39(1): p. 165-184.

[4]. S. Zhang, *et al.*, A methodology for obtaining material properties of polymeric foam materials at elevated temperatures. Submitted to Experimental mechanics, 2011.

[5]. DIAB, Divinycell PVC datasheet. http://www.diabgroup.com, 2010.